LABORATOIRE DE PHYSIQUE CORPUSCULAIRE

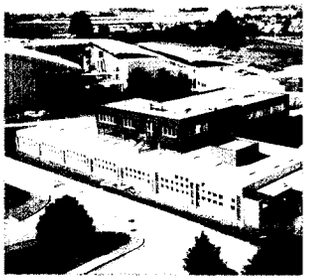

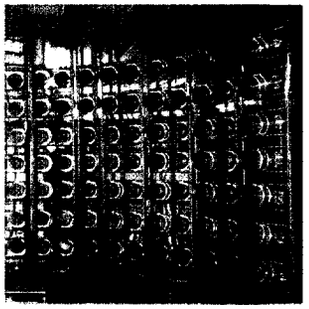

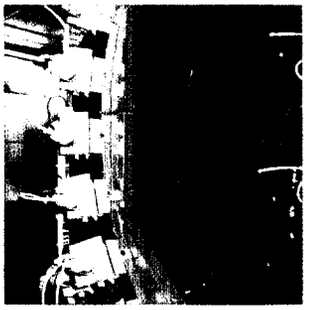

TIME DEPENDENCE OF THE MULTIFRAGMENTATION PROCESS IN 50 A.MeV Xe+Sn REACTIONS

R. Bougault, J.P. Wieleczko, M. D'Agostino, W.A. Friedman, N. Le Neindre, F. Gulminelli, A. Chbihi, S. Salou, G. Auger, C.O. Bacri, N. Bellaize, F. Bocage, B. Borderie, R. Brou, P. Buchet, J. Colin, D. Cussol, R. Dayras, A. Demeyer, D. Doré, D. Durand, J.D. Frankland, E. Galichet, E. Genouin-Duhamel, E. Gerlic, D. Guinet, P. Lautesse, J.L. Laville, J.F. Lecolley, R. Legrain, O. Lopez, M. Louvel, A.M. Maskay, L. Nalpas, A.D.N'Guyen, M. Pârlog, J. Péter, E. Plagnol, M.F. Rivet, E. Rosato, F. Saint-Laurent, J.C. Steckmeyer, M. Stern, G. Tabacaru, B. Tamain, L. Tassan-Got, O. Tirel, E. Vient, C. Volant
(INDRA Collaboration)

February 1999 LPCC 99-06

Contributed paper to International Workshop xxvII on Gross Properties of Nuclei and Nuclear Exitations Waldemar-Petersen-Haus, Hirschegg, Kleinwalsertal (Austria), 17-23 january 1999

CENTRE NATIONAL DE LA RECHERCHE SCIENTIFIQUE

INSTITUT NATIONAL
DE PHYSIQUE NUCLÉAIRE ET DE PHYSIQUE DES PARTICULES

INSTITUT DES SCIENCES DE LA MATIÈRE ET DU RAYONNEMENT

UNIVERSITÉ DE CAEN

- U.M.R.6534 -
ISMRA - 6, Boulevard Maréchal Juin - 14050 CAEN CEDEX - FRANCE

Téléphone : 02 31 45 25 00 - Télécopie : 02 31 45 25 49
Internet : http://caeinfo.in2p3.fr

CNRS CENTRE NATIONAL DE LA RECHERCHE SCIENTIFIQUE IN2P3 ISMRA

TIME DEPENDENCE OF THE MULTIFRAGMENTATION PROCESS IN 50 A.MeV Xe+Sn REACTIONS[1]

R. Bougault[a], J.P. Wieleczko[b], M. D'Agostino[a],[2], W.A. Friedman[b],[3], N. Le Neindre[a],F. Gulminelli[a], A. Chbihi[b], S. Salou[b], G. Auger[b], C.O. Bacri[c], N. Bellaize[a], F. Bocage[a], B. Borderie[c], R. Brou[a], P. Buchet[d], J. Colin[a], D. Cussol[a], R. Dayras[d], A. Demeyer[e], D. Doré[d], D. Durand[a], J.D. Frankland[c], E. Galichet[e], E. Genouin-Duhamel[a], E. Gerlic[e], D. Guinet[e], P. Lautesse[e], J.L. Laville[b], J.F. Lecolley[a], R. Legrain[d], O. Lopez[a], M. Louvel[a], A.M. Maskay[e], L. Nalpas[d], A.D. N'Guyen[a], M. Pârlog[f], J. Péter[a], E. Plagnol[c], M.F. Rivet[c], E. Rosato[g], F. Saint-Laurent[b],[4], J.C. Steckmeyer[a], M. Stern[e], G. Tabacaru[f], B. Tamain[a], L. Tassan-Got[c], O. Tirel[b], E. Vient[a] and C. Volant[d]

(INDRA collaboration)

[a] *Laboratoire de Physique Corpusculaire, IN2P3-CNRS, ISMRA et Université, F-14050 Caen cedex, France*

[b] *Grand Accélérateur National d'Ions Lourds, DSM-CEA/IN2P2-CNRS, BP 5027, F-14076 Caen cedex 5, France*

[c] *Institut de Physique Nucléaire, IN2P3-CNRS et Université, BP 1, F-91406 Orsay cedex, France*

[d] *DAPNIA/SPhN, CEA/Saclay, Orme des Merisiers, F-91191 Gif-sur-Yvette cedex, France*

[e] *Institut de Physique Nucléaire, IN2P3-CNRS et Université, F-69622 Villeurbanne cedex, France*

[f] *National Institute for Physics and Nuclear Engineering, RO-76900 Bucharest-Magurele, Romania*

[g] *Dipartimento di Scienze Fisiche e Sezione INFN, Università di Napoli "Federico II", I-80126 Napoli, Italy*

---

[1] Experiment performed at Ganil

[2] on leave from : Dipartimento di Fisica and INFN, Bologna, Italy

[3] on leave from : Department of Physics, University of Wisconsin, Madison, USA

[4] present address : DRFC/STEP, CEA/Cadarache, Saint Paul lez Durance, France

Abstract

The Xe+Sn 50 A.MeV one source events are confronted with SMM calculations. An excellent agreement on the mean values of several observables extracted from fragment characteristics is found if the mass and the excitation energy of the multifragmenting source are reduced as compared to experimental data. Furthermore an extra mean collective energy of 2 A.MeV is needed at the break-up time in order to explain the mean fragment kinetic energies. These facts are confirmed by EES and BNV calculations which indicate that the measured collective energy arises from compression of the nuclear matter and that multifragmentation occurs after an expansion process where excitation energy and mass are lost by the hot and compressed source before its break-up. The fragment characteristics inform on the break-up of the source while the light particles, whose characteristics agree with EES-prediction, are produced at several steps of the expanding multifragmentation process.

1 Introduction

The fascinating process, referred as nuclear multifragmentation focuses many experimental and theoretical works [1, 2, 3, 4, 5] [6, 7, 8, 9] since it provides information on properties of excited nuclear matter at subnormal densities and may signal a liquid-gas phase transition in finite nuclear systems. In this context, exploration of central collisions of heavy systems is fundamental [10, 11, 12, 13, 14] since it is believed that, for suitable bombarding energy, a high density is reached in the early stage of this kind of reactions. From such studies one expects valuable information to answer the question whether or not compression induces a specific pattern for multifragmentation. However, the understanding of the complex evolution of these collisions, from an early non-equilibrium and eventually compressed stage to a late fragmentation stage through an expansion process possibly influenced by dynamical effects, remains a great challenge and demands careful investigations. The fundamental issue is whether or not an equilibrated system is created in the course of the collision. This is essential to extract valid information on the thermodynamical properties of highly excited nuclear matter, and ultimately to determine its equation of state.

2 Single source events

In a previous work [12], we have reported on the study of the multifragmentation process in central Xe+Sn collisions detected with the large acceptance 4π

detector INDRA [15, 16, 17]. In this contribution, we will present further analysis on the same set of data. Let us recall the main results of [12]. A first data selection was performed by imposing for each event a completeness criterion, i.e. the sum of the total detected charge exceeds 80% of the combined charge system. On this sample we have performed an event by event shape analysis based on the 3-dimensional kinetic energy flow tensor calculated in the center-of-mass frame of the reaction. Only fragments with $Z \geq 3$ were included for the calculation of the tensor which is thus as much as possible independent of secondary decay and preequilibrium effects. We have defined the angle Θ_f between the beam axis and the eigenvector associated to the largest eigenvalue of the diagonalized tensor. A selection of events with $\Theta_f \geq 60°$ allows one to isolate a sample where most of the charged products are emitted from a single source indicating that a high degree of equilibration has been reached in the selected collisions. The source so isolated had an estimated total charge of 90 (taking into account the detector efficiency) and an estimated mean excitation energy of about 12 A.MeV. Finally, a quantitative analysis, by means of a phenomenological model, of the kinetic energy of the fragments indicated the simultaneity of the disintegration process and the need for an extra collective radial motion of about 2 A.MeV superimposed onto the thermal and Coulomb components. For more details, see reference [12].

The points we want to address here are the following : (i) to confront our previous findings to a statistical multifragmentation model and to extract mean characteristics of the multifragmenting source, (ii) to relate the collective energy ($E_{\rm coll}(\rho, T)$) directly to compression effects or/and to a thermal expansion caused by the thermal pressure, and (iii) finally to propose a scenario connecting the previous points. For this purpose, we will first concentrate on fragment characteristics. Light charged particle (lcp) properties [18] will be used to validate the proposed scenario.

3 Confrontation to SMM

We have compared the experimental data with the prediction of the Statistical Multifragmentation Model (SMM) [19, 20] used in a modified version [20] which includes the presence of an extra collective radial expansion at the freeze-out. In this version, the self-similar extra collective motion does not interfere with the thermodynamical procedure of partition generation. Calculations presented here have been performed with a freeze-out density one third of nuclear saturation density (i.e $\rho_0/3$). Simulated events were filtered with the detector acceptance and analysed as the data were. In data-model confrontation one

compares variables which must be representative of the sample. A way to do so is to choose in the data and the generated sample a group of events which represents the most probable behaviour of the experimental findings and of the model predictions. It is obvious that the size distribution of the fragments in an event depends on the fragment multiplicity. Therefore for the studied sample the shape of the fragment size distribution, especially in the large-size region, is not representative of the most probable event but rather reflects the weight of low fragment multiplicity events in the sample. To remove this problem we have chosen to perform a cut in the multiplicity of fragments with $Z \geq 4$ ($M(Z \geq 4)$ in fig. 1-a). The representative sample will be chosen by retaining the events leading to a value of 5 or 6 (most probable values : grey area fig. 1-a) for $M(Z \geq 4)$. This choice ($M(Z \geq 4)$=5 or 6) was governed by a compromise between good statistics, agreement between mean value and most probable value for the variable and a selection linked to a direct measurement rather than based on a calculated variable. This choice ensures a relevant meaning and description for all observables presented in this letter. The same choice ($M(Z \geq 4)$=5 or 6) has been performed for SMM calculations after the filter procedure, the completeness criterion and the $\Theta_f \geq 60°$ selection.

An SMM-calculation assuming a source size of $Z_s(\rho_0/3) = 90$ and a total excitation energy of 12 A.MeV with 2 A.MeV corresponding to an extra collective radial motion (i.e. 10 A.MeV for partition generation) fails to explain the data. Then several calculations were performed following a method similar to the one used in [11]. The charge and the excitation energy at the freeze-out are determined by taking them as adjustable parameters so as to reproduce at best the data. The mass of the source is determined by the N/Z-ratio of the Xe+Sn system. The observables chosen as references are (i) the mean fragment multiplicity (including Z=3), (ii) the mean charge bound in fragments (including Z=3), (iii-vi) the mean sizes of the four biggest fragments. The extra collective energy ($E_{coll}(\rho_0/3)$) has not been used as an adjustable parameter but rather was set so to reproduce the mean c.m energies of IMF's. Finally a χ^2-test taking the data as reference was used. When superimposing the six χ^2 in a plot of excitation energy versus charge of the source a clear minimum is found. In the data-model comparison, the size of the biggest fragment plays the major role in extracting the excitation energy, while multiplicity of lighter IMF governs the source charge. From the confrontation with the data, it results that SMM can reproduce the mean experimental features for a source size of $Z_s(\rho_0/3) = 80$ and $E^*(\rho_0/3) = 9$ A.MeV, from which 2 A.MeV are bound in extra collective energy ($E_{coll}(\rho_0/3) = 2$ A.MeV). As it can be seen on fig. 1-b and 1-c the agreement is excellent.

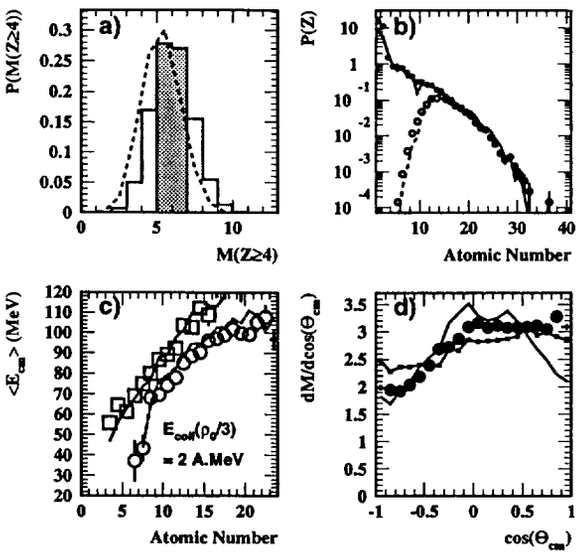

Figure 1: *Data (dots or squares) and SMM-calculation (lines) with* $E_{\rm coll}(\rho_0/3) = 2$ *A.MeV.* **a)** Fragment ($Z \geq 4$) multiplicity : all the selected data (histogram) compared with SMM-calculation (dashed line) which reproduces the experimental most probable event as defined by the grey area. **b)** Most probable event : Z-distribution (black dots and line) and size of the biggest-fragment (open dots and dashed line). **c)** Most probable event : c.m mean kinetic-energy for $Z \geq 3$ fragments; for the biggest fragment (dots and line) and for all but the biggest fragment (squares and line). **d)** Most probable event : c.m angular distribution of the fragments ($Z \geq 4$); data (dots) is compared with SMM-calculation selected with (line) and without (line with small black squares) the $\Theta_{\rm f}$ criterion.

The check of relevance of SMM-result is presented on fig. 1-a (dashed line) where it is shown that the experimental average multiplicity does correspond to the calculated averaged multiplicity within the RMS. The c.m angular distribution for fragments ($Z \geq 4$) is presented in fig. 1-d. It is compared with SMM prediction filtered with and without the $\Theta_{\rm f} \geq 60°$ cut. From this picture we see that an isotropic distribution is deformed by the detection efficiency in the backward hemisphere. We see also that the $\Theta_{\rm f}$ cut selects, within an isotropic distribution, the events which energetically flow preferentially per-

pendicular to the beam axis. The discrepancy between data and model is weak and essentially limited to forward angles and thus does not alter our conclusions. The kinetic energies of the fragments put a severe constraint on the model as they reflect the contributions of thermal, Coulomb and an eventual extra radial collective energy. In fig. 1-c, we report the Z dependence of the mean values of the c.m kinetic energy spectra of the largest fragment in each event and of the other fragments. A calculation with $Z_s(\rho_0/3) = 80$ and $E^*(\rho_0/3) = 7$ A.MeV fails to explain the kinematic observables. A clear improvement is observed when an extra collective radial energy ($E_{coll}(\rho_0/3)$) of 2 A.MeV is added. This value of 2 A.MeV is in agreement with our previous finding [12] and the SMM-calculation is now consistent with the data in absolute values and trends of both profiles.

The multiple production of fragments associated to the disintegration of the single source formed in central Xe+Sn collisions at 50 A.MeV is consistent with the Statistical Multifragmentation Model. This is a strong indication that at the disintegration stage of the reaction a thermodynamical equilibrium has been reached (the same conclusion has been achieved in a previous work using lcp-IMF correlations [21]). SMM has also been used to extract mean conditions at the freeze-out time (mass and excitation energy). In the model the fragment configurations are calculated first and depend on the thermal energy only, then the extra collective flow is introduced. This procedure is based on the assumption that thermal degrees of freedom and extra collective radial motion are decoupled. This decoupling hypothesis agrees at first order with data.

4 Collective energy

The relevance of angular momentum to explain the data behaviour is ruled out when comparing the azimuthal correlations of lcp [12]. The question whether or not the measured extra collective energy is directly connected to compression effects or can be partly due to thermal pressure will now be addressed. In order to disentangle the thermal and compression parts of the measured extra collective energy at freeze-out, we have performed EES-calculations [22] for the 50 A.MeV Xe+Sn system. The input values for the EES calculations are the experimental estimates (A=214, Z=90, E^*=12 A.MeV). The Expanding Emitting Source model follows the time evolution of a heated nucleus. It assumes that the initial equilibrated system, once heated, expands isentropically from nuclear saturation density (ρ_0). The evolution of the system depends upon the thermal pressure which makes the nucleus expand and the nuclear

forces which react against the expansion. Therefore the collective energy is a function of time. The maximum value is reached at a density slightly lower than ρ_0 then $E_{\rm coll}$ decreases. If the initial temperature is low $E_{\rm coll}$ eventually vanishes and the system will be driven back towards ρ_0. For large temperatures, the heated nucleus will expand towards low densities. The source emits particles and fragments during the expansion phase and the time dependent emission rates of the species are calculated within the statistical Weisskopf surface emission formalism. There is a strong coupling between the mass and the density (ρ) of the expanding source, as the mass decreases, ρ decreases. There is also a strong coupling between the density and the rate of emission. When the system eventually reaches the cross-over point where the free energy for producing a free particle is equal to the free energy for producing a particle inside the volume, surface emission does not make sense any more and the model switches to volume emission. This well defined point corresponds to a density of approximately $\rho_0/3$ and is responsible for changes of kinematical features and for large production of Intermediate Mass Fragments (IMF) which are not copiously produced in the surface emission phase (about 20% for this system). For technical reasons, only fragments with $Z \leq 9$ are considered in the model. First we have performed a standard calculation. In this case the expansion is governed by thermal pressure alone. In such conditions, the system indefinitely expands towards low densities, meaning that at 12 A.MeV excitation energy no compression is a priori needed to explain the occurrence of multifragmentation. The whole process yields numerous IMF's with charge ≤ 9 with a mean multiplicity compatible with the experimental one when considering the same element range. In fig. 2-a, we compare the calculated (labelled 0 A.MeV) and measured mean kinetic energy of the different elements. The calculation clearly underestimates the measured fragment kinetic energies. This excludes a purely thermal origin for the extra collective motion observed in the data. Then another calculation was performed assuming an initial collective radial energy stored in the system at ρ_0. This extra collective radial energy at ρ_0 can be here considered as a pure compression effect since it assumes implicitly that the source was formed at a density greater than ρ_0. This compression energy reduces the thermal excitation energy of the source since in the calculation the total excitation energy is kept equal to 12 A.MeV. An initial collective energy at ρ_0 of 2.5 A.MeV allows to well account for the experimental data (fig. 2-a). For this calculation, we still observe an expansion towards low densities without stopping (atomic number and density of the source in fig. 2-b). In these conditions the model predicts at $\rho_0/3$ an atomic number of the source (fig. 2-b) and a residual collective energy ($E_{\rm coll}(\rho_0/3) = 2.3$ A.MeV) close to

the values obtained with SMM.

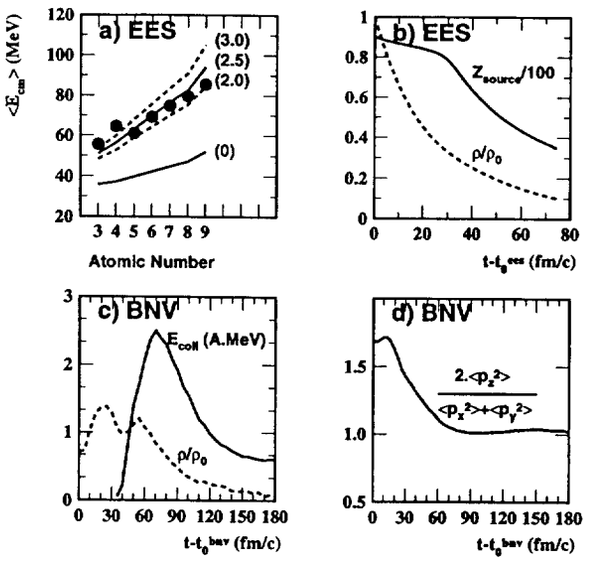

Figure 2: *EES (top)* : **a)** : mean c.m kinetic-energy of IMF's for data (points) and EES-calculations with four different initial collective energy at ρ_0; **b)** : density and charge of the source as a function of time for a calculation with an initial collective energy of 2.5 A.MeV at ρ_0. *BNV-calculation at b=0 fm (bottom)* : **c)** density and collective energy as a function of time; **d)** : isotropy ratio in the momentum space as a function of time (z is the beam axis).

With EES-calculations, we have shown that the measured collective energy in the selected central 50 A.MeV Xe+Sn collisions corresponds to compression effects. Furthermore due to the evolutionary nature of the EES-modelization, global properties of the system such as mass, density, collective energy can easily be followed during the process. When looking at the characteristics of the system given by EES-calculation at the "force-freeze-out" point ($\rho_0/3$), we found them close to the freeze-out conditions deduced from the SMM-calculation. The extraction of mean conditions at the freeze-out time from fragments characteristics is not affected by the weak IMF-production during the surface evaporation process.

5 Expanding multifragmenting source

We will now compare our results with a transport model calculation which takes into account the entrance channel. It will be used to quantify our results in term of fundamental variables as for example maximum achieved density. In the model, the collision is followed by solving the BNV equation with a numerical technique based on a test particle approach [23]. The dynamics is governed by the competition between mean field effects and two body collisions. In the calculation, the nuclear part of the mean field is approximated by a density dependent Skyrme force with an incompressibility modulus of 200 MeV, and the nucleon-nucleon cross section is assumed to be the energy, angle and isospin dependent free one. In figs. 2-c and 2-d are presented some results for head-on (b=0 fm) 50 A.MeV Xe+Sn collisions. For this system, a source whose center coincides with the c.m is formed and its time evolution has been extracted by considering as unbound the nucleons located in regions where the local density is less than 1/10 of the nuclear saturation density (i.e. $\rho_0/10$). The time evolution of the reaction is shown in fig. 2-c (time t=0 corresponds here to projectile and target at contact). First, a compression stage occurs which, after a first density maximum exhibits a density oscillation due to a competition between ingoing and outgoing particles during the pressure build-up (rarefaction wave). The second maximum in density is reached when the two partners fully overlap. In the second stage the system starts to expand and reaches ρ_0 around 65 fm/c. At that time the thermal equilibrium of the system is achieved : this stands out from fig. 2-d where is presented the isotropy in the momentum space as a function of time. Since the mean-field tends to restore nuclear media towards nuclear saturation density, about at the same time the radial energy ($E_{\rm coll}$) reaches a maximum value (fig. 2-c) in quantitative agreement with the one deduced from EES-calculation. From this time on the expansion is roughly isentropic and at about 90 fm/c the dilute system enters the spinodal region (calculated for infinite nuclear matter) with a reduced radial energy comparable to the ones deduced from EES and SMM calculations. If one thinks that at that point fluctuations increasingly develop [24], then the calculation does not give the correct subsequent behaviour because in the spinodal region a mean-field calculation loses its validity. We do see that the time needed (about 30 fm/c) by the system to expand from ρ_0 to $\rho_0/3$ is compatible with the EES-calculation. Then BNV and EES calculations indicate that the source loses mass and energy before reaching the freeze-out stage. This explains the necessity to reduce the excitation energy and the mass of the source in SMM-calculation in order to reproduce the experimental

fragment characteristics.

6 Confirmation with light charged particles

The analysis of lcp originating from the multifragmenting source is done by selecting only lcp emitted around 90° in the c.m ($-0.5 \leq cos\Theta_{cm} \leq 0.5$). The anisotropic lcp-component, not discussed here, is forward/backward peaked [12]. In Fig. 3, the lcp c.m kinetic energy spectra and their mean values are

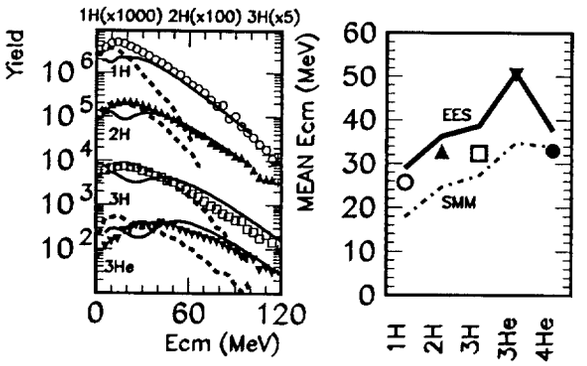

Figure 3: *Light charged particle characteristics for data (markers :* $-0.5 \leq cos\Theta_{cm} \leq 0.5$*), SMM (dashed-lines :* $-0.5 \leq cos\Theta_{cm} \leq 0.5$*) and EES (solid-lines)* : **left)** : c.m kinetic-energy spectra, **right)** : c.m mean kinetic-energy.

presented. The prediction of the multifragmentation model SMM is also shown in both pictures and apart for alpha-particles the SMM-calculation which reproduces the fragment mean characteristics is unable to describe properly the lcp features. In particular, the "puzzling" energy spectra of ^3He [25, 26, 27, 18] is not reproduced by SMM-prediction. In the SMM-model lcp's originate from the freeze-out configuration and from secondary decay of primary excited clusters. In order to take into account the time evolution of the multifragmentation process, we have calculated the lcp's energies within the EES-scenario. The input parameters of the model are those which lead to agreement with the fragment characteristics for the studied system as quoted above. The result for c.m energies is presented in Fig. 3. A general qualitative agreement is

achieved. The mean energy of Z=2 particles are reproduced, and especially the ^3He puzzle does not seem to be a puzzle any more. The good agreement with EES is due to the occurrence of particle emission during the expansion phase which is not in the basic physics of SMM whose starting point is a low density freeze-out configuration. EES-energy spectra for lcp's are presented in Fig. 3. The spectra can be divided in two parts which corresponds to surface (high energy) and volume (low energy) emission. The dip at low kinetic energy is the result of the sharp switch from surface to volume emission and lack of secondary recoils. Also in EES-model the calculation is stopped at $\rho_0/10$ and therefore one does not expect to fully explain the very low energy part of lcp's. Nevertheless, as seen in those spectra, surface emission is properly selected by a cut in energy at about 60 MeV. Precisely those particles which are not reproduced by the SMM-calculation.

As a conclusion, when considering that the high energy part of lcp production is governed by emission during the expansion phase we can explain both lcp and fragments characteristics within a time dependence scenario for the multifragmentation process.

7 Conclusion

To conclude, firstly it has been shown that the collective energy measured in 50 A.MeV Xe+Sn one-source events is mainly associated to compression effects. Indeed a dynamical calculation reveals that the nuclear system has reached a maximum density of about 1.2 nuclear saturation density. Secondly the multifragmentation process can be explained within an evolutionary scenario. This evolution is understood if one considers that the compressed system expands and reaches the freeze-out point after losing mass and excitation energy. This scenario is confirmed by lcp characteristics. Finally, the data mean characteristics can be explained in the framework of thermodynamical equilibrium.

One of the authors (MDA) would like to thank the LPC for the kind hospitality and financial support.

References

[1] B. Tamain and D. Durand, Multifragmentation of Nuclei, in: H. Nifenecker, J.-P. Blaizot, G.F. Bertsch, W. Weise and F. David eds., *UJFG LES HOUCHES session LXVI, trends in nuclear physics 100 years latter* (Elsevier, 1998) 295.

[2] G.F. Peaslee et al., Phys. Rev. **C49** (1994) R2271.

[3] A.J. Cole et al., Z. Phys. **A356** (1996) 171.

[4] Hongfei Xi et al., Z. fur Physik **A359** (1997) 397.

[5] L.G. Moretto et al., Phys. Rep. **287** (1997) 249.

[6] W. Reisdorf et al., Nucl. Phys. **A612** (1997) 493.

[7] G. Wang et al., Phys. Rev. **C57** (1998) R2786.

[8] P. Désesquelles et al., Nucl. Phys. **A633** (1998) 547.

[9] S.P. Avdeyev et al., Eur. Phys. J. **A3** (1998) 75.

[10] D.R. Bowman et al., Phys. Rev. **C46** (1992) 1834.

[11] M. D'Agostino et al., Phys. Lett. **B371** (1996) 175.

[12] N. Marie et al., Phys. Lett. **B391** (1997) 15.

[13] W. Reisdorf and H.G. Ritter, Annu. Rev. Nucl. Part. Sci. **47** (1997) 663.

[14] M.F. Rivet et al., Phys. Lett. **B430** (1998) 217.

[15] J. Pouthas et al., Nucl. Instrum. Methods **A357** (1995) 418.

[16] J.C. Steckmeyer et al., Nucl. Instrum. Methods **A361** (1995) 472.

[17] J. Pouthas et al., Nucl. Instrum. Methods **A369** (1996) 222.

[18] R. Bougault et al., A possible scenario for the time dependence of the multifragmentation process in Xe+Sn collisions (an explanation of the 3He puzzle), in: I.Iori ed., *Proceedings of the XXXV International Winter Meeting on Nuclear Physics* (Bormio, 1997) 251.

[19] A.S. Botvina et al., Nucl. Phys. **A475** (1987) 663.

[20] J.P. Bondorf, A.S. Botvina, A.S. Iljinov, I.N. Mishustin and K. Sneppen, Phys. Rep. **257** (1995) 133.

[21] N. Marie et al., Phys. Rev. **C58** (1998) 256.

[22] W. A. Friedman, Phys. Rev. **C42** (1990) 667.

[23] A. Bonasera, F. Gulminelli and J. Molitoris, Phys. Rep. **243** (1994) 1.

[24] P. Chomaz, Ann. Phys. **21** (1996) 669.

[25] K.G.R. Doss et al., Mod. Phys. Lett. **A3** (1988) 849.

[26] G. Poggi et al., Nucl. Phys. **A586** (1995) 755.

[27] M.A. Lisa et al., Phys. Rev. Lett. **75** (1995) 2662.